

Article

Revealing Impacts of Trees on Modeling Microclimate Behavior in Spaces between Buildings through Simulation Monitoring

Lirui Deng ¹, Xibei Jia ¹, Wei Wang ^{1,*} and Syed Asad Hussain ^{2,*} ¹ School of Architecture, Southeast University, Sipailou 2#, Xuanwu District, Nanjing 210096, China² Life Cycle Management Laboratory (LCML), School of Engineering, The University of British Columbia, Vancouver, BC V6T 1Z4, Canada

* Correspondence: weiwang@seu.edu.cn (W.W.); asad.hussain@ubc.ca (S.A.H.)

Abstract: Urban trees have been recognized as having different impacts on the microclimate and thermal comfort. Therefore, this study conducted on-site measurement and simulation to explore and clarify how trees impact the microclimate, thermal comfort, and façade temperature. A campus site was selected as the test field and two models—one with and one without trees—were built with the ENVI-met. Meanwhile, one microclimate station and four sensors were installed to simulate and validate the microclimate. Twelve blocks with different tree conditions were also selected to further investigate the specific impacts of trees. The results showed that, firstly, the transpiration and sheltering effect of trees that dominates on sunny days can decrease air temperature and the predicted mean vote. Secondly, trees' effects on airflow, including on the wind channel and blocking effect, are dominant on cloudy days. Trees inside the group often exhibit the wind-blocking effect, while trees with a downwind determinant at the windward group edge usually exhibit the wind channel effect. Thirdly, high canopy coverage enhances trees' sheltering effect on solar radiation. The study also provides design recommendations for campus building and trees that account for how trees help improve the microclimate, enhance comfort, and reduce energy consumption.

Keywords: impacts of trees; microclimate behavior; outdoor thermal comfort; façade temperature; simulation-measurement approach



Citation: Deng, L.; Jia, X.; Wang, W.; Hussain, S.A. Revealing Impacts of Trees on Modeling Microclimate Behavior in Spaces between Buildings through Simulation Monitoring. *Buildings* **2022**, *12*, 1168. <https://doi.org/10.3390/buildings12081168>

Academic Editor: Alessandro Cannavale

Received: 3 July 2022

Accepted: 3 August 2022

Published: 4 August 2022

Publisher's Note: MDPI stays neutral with regard to jurisdictional claims in published maps and institutional affiliations.



Copyright: © 2022 by the authors. Licensee MDPI, Basel, Switzerland. This article is an open access article distributed under the terms and conditions of the Creative Commons Attribution (CC BY) license (<https://creativecommons.org/licenses/by/4.0/>).

1. Introduction

With China's rapid urbanization and economic growth, the urbanization rate in China reached 64.72% until 2021 [1]. Beyond promoting urban development and an improved quality of life, urbanization causes a series of negative effects, such as the deterioration of the environment and the gradual fragility of the ecology [2]. These effects not only lead to human health issues and climate change, but also impact energy use and carbon emissions [3]. Specifically, rapid urbanization poses urban thermal challenges with a range of environmental consequences, including increased difficulty for people to participate in outdoor activities [4], increased storms and precipitation events [5], and increased heat-related mortality [6]. The urban heat island effect (UHI) is a phenomenon of urban thermal challenges where high surface or air temperatures occur more often in urban areas than in the suburbs [7]. UHI negatively impacts human society and urban life and is not conducive to sustainable urban development. The key to mitigate the heat island effect at the neighborhood level lies in studying how to improve the urban microclimate.

Microclimate behavior, as a climate phenomenon in the complex urban context, is inseparably related to urban air quality and livability, but many other indicators also affect the microclimate, such as urban and building morphology [8], urban greening [9] (e.g., trees and vegetation), and artificial landscape. In shaping the urban microclimate, many studies have attempted to reveal the important role of urban and architectural morphological parameters [10,11]. Bouketta and Bouchahm studied the effects of urban

geometry on airflow and found enclosed spaces such as L-shaped buildings could cause poor ventilation [12]. In addition, microclimates in urban canyons are influenced by height-to-width (H/W), length-to-width (L/W), and length-to-height (L/H) ratio, as well as by street orientation [13]. Muniz-Gaal et al. found that canyons with a higher H/W aspect ratio increased the wind speed and shading, thereby improving thermal comfort at the pedestrian level in the summer, while an increase in the L/H ratio had no significant effect on thermal comfort [14]. Moreover, Hang et al. found that street length had no significant effect on wind flow capacity, in contrast to canyon width [15]. Tong et al. proposed that the microclimate is affected by the sky view factor (SVF) [16]. The measurement in Sydney proved that, on the one hand, the daily average wind speed was spatially proportional to SVF, but on the other hand, high SVF led to a high daily average air temperature [17].

Another determinant of the microclimate is the urban greening, including trees, vegetation, water, and artificial landscape. With ENVI-met software (v.4.4.6, Bruse Team, Essen, Germany), Li and Song combined in situ measurements and a three-dimensional microclimate model to examine microclimate variations in an urban neighborhood park [18]. Armson et al. [19] explored the roles of trees and grass in reducing regional and local temperatures, finding that increasing vegetated area and strengthening green infrastructure will decrease the air temperature and reduce heat. Generally, urban vegetation is known to create shade and cool the environment [20,21], and tree species, leaf density, and branch structure are especially decisive [22], but not all situations with trees can significantly reduce the cooling energy loads. The effects of shading and cooling depend on the distance of trees from buildings and the available space for trees [23]. The studies mentioned above mainly discovered how trees and plants could change air temperature, but both could also reduce wind speed and change wind direction, thereby affecting the urban microclimate [24]. Other urban landscape elements, such as water [25] and the albedo of surface material [26], contribute to shaping microclimate as well. Additionally, a good climatic effect of vegetation can be achieved with sufficient irrigation, which results in additional water requirements. Well and Ludwig claimed that setting up fountains or artificial wetlands could improve the microclimate in conjunction with urban greening—that is, the Blue-Green method interlinking blue and green aspects [27].

Previous studies have proved a strong correlation between the microclimate and thermal comfort [28,29], and many considered air temperature and solar radiation as the two microclimate parameters most relevant to human comfort [30,31]. Reciprocally, the height and thermal performance of walls affect the microclimate, and solar radiation and urban structure are the most important determinants of thermal environment [32]. Xu et al. investigated thermal comfort during winter in different urban park landscapes in Xi'an and proposed solar radiation as the most important aspect and wind speed as the least important [33]. Nikolopoulou and Lykoudis [34] emphasized that high wind speed may exacerbate discomfort, and that wind speed only needs to be raised in hot conditions. In sum, improving the microclimate through urban form and vegetation optimization will promote human comfort and ameliorate city livability. According to [35], strengthening urban greening is conducive to improving the thermal environment and reducing energy consumption. The degree of thermal comfort improvement, however, depends on the tree species and morphological structure of vegetation [36,37]. Morakinyo et al. found leaf area index, tree height, and trunk height to most impact improving the outdoor thermal comfort in Hong Kong [38]. Hsieh et al. [39] and Xu et al. [40] proposed that these effects were mainly produced by shadows from the shading radiation and transpiration of plants but noted that wind blocking may also be influenced. Shashua-Bar et al. calculated trees' cooling effect by comparing air temperature in the street with and without trees, ultimately concluding that canopy cover determines the cooling effect of trees on streets [41]. Sabrin et al. also studied the effect of existing (with and without) vegetation on thermal comfort in five cases and found that planting trees in residential and mixed-use sites with higher SVF could improve pedestrian comfort [42]. Finally, the improvement in microclimate

facilitated by vegetation is thought to affect the exterior wall temperature of buildings, which must change the indoor environment and energy consumption [43].

Therefore, urban greening plays a significant role as a key part of modern cities. Several studies have indicated multiple impacts of green plants. For example, in sunlit areas, trees can shield solar radiation and reduce heat storage, but can also block airflow and decrease wind speed [44,45]. Tan et al. discussed the effects of increased vegetation area on the microclimate and the application of tree planning strategies to alleviate the urban heat island under certain conditions [46]. Abdi et al. explored how street trees affect the microclimate, correlating with location, tree species, density, and orientation of the rows related to prevailing winds [47]. Zhao et al. studied the impacts of trees height on the façade temperature of enclosed courtyard in North China [48]. Considering that the exterior building walls are a bridge between the indoor and outdoor environment, the microclimate will inevitably affect the indoor environment and energy consumption.

Above all, numerous studies illustrated the urban trees have different types of impacts on microclimate behavior, comfort, and façade temperature, including the shading effect of trees, transpiration, and the effect on airflow. However, most researchers analyzed the cooling effect of the shadows generated by trees shading the solar radiation and transpiration on the urban underlying surface. Only a few researchers emphasized how trees affect airflow and changes in wind speed, but ignored multiple ways that trees impact the façade temperature, microclimate behavior, and thermal comfort in spaces between buildings. Researchers further ignored what consequences different impacts will have and which impact will be in a dominant position under what circumstances and under seasonal differences. To answer such questions, this study used a university campus as the case area and applied the microclimate analysis software ENVI-met (v.4.4.6, Bruse Team, Essen, Germany) for modeling and simulation with on-site measurements to validate the model reliability. By using the simulation results to analyze the differences among different seasons, different amounts of solar radiation and different tree layouts, this study aims to finally reveal the specific mechanism of trees that improves the urban environment and changes the façade temperature. The findings also provide valuable references on how to plant trees and respond to different seasons and weather conditions in building design and performance optimization.

2. Methodology

2.1. Overview of the Methodology

Figure 1 presents the framework this study used to investigate the impacts of urban trees on the microclimate behavior between buildings, thermal comfort, and façade temperature. The research methodology is field measurement and numerical simulation. Through on-site measurement, we obtained the required meteorological parameters to generate the weather file for microclimate simulation, and four distributed environmental sensors were allocated in the Southeast University Campus to generate ground truth to validate the microclimate experiment. Numerical simulation was carried out using ENVI-met (v.4.4.6, Bruse Team, Essen, Germany), and basic model settings include buildings, vegetation, single walls, soil, and surface. Two scenarios—tree and treeless campus models—were established to compare and analyze microclimate behaviors (e.g., temperature, wind speed, and relative humidity), as well as their impact on the thermal comfort with the predicted mean vote (PMV) and building façade temperature. Eventually, this study discussed and compared several different ways trees improve urban livability by optimizing the microclimate and influencing the building façade.

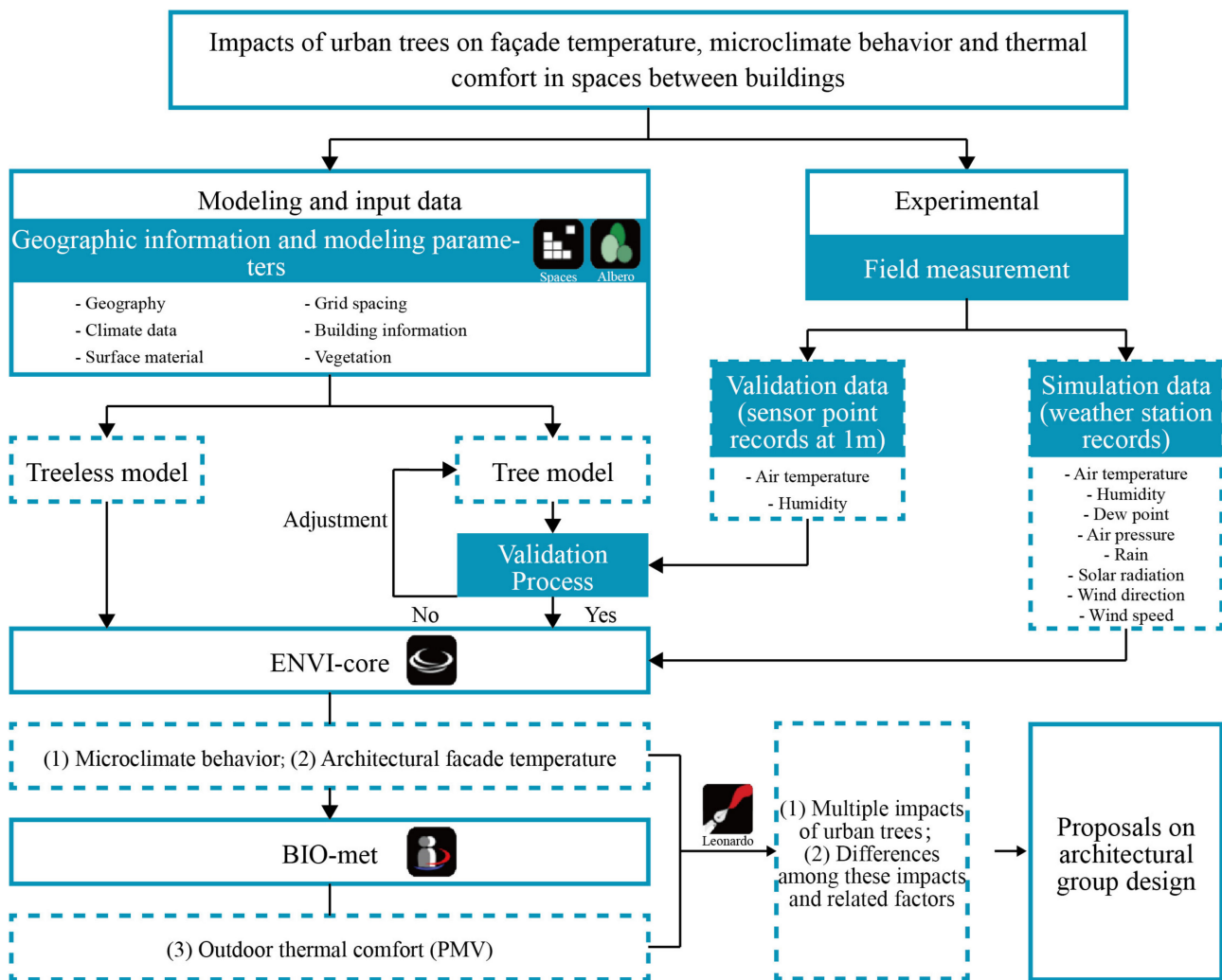


Figure 1. Framework of research method used in this study.

2.2. Case Area

We selected the Sipailou Campus of Southeast University (SEU) as the research case area, located in Nanjing, Jiangsu Province in the lower reaches of the Yangtze River in southeastern China, bordering the Yangtze River Delta to the east. Figure 2 presents the location of Nanjing, the SEU campus, and a bird's eye view. The SEU campus covers 411,309 m², and the total construction area is 476,587 m². SEU is also listed as a national key cultural heritage protection unit by the State Council of China and was selected for the "First Batch of China's 20th Century Architectural Heritage" list in September 2016. The orderly and well-proportioned building complex is symmetrically arranged in the north-south direction, mostly decorated with ionic columns in the foyer and reinforced concrete and brick-wood structures, built mainly in the 1920s and 1930s. As shown in Figure 2, the greening resources on campus are very rich, and the overall greening rate reaches 39.8%. Various tree species—including platanus, pine, cypress, metasequoia, and cherry blossoms—are present on campus. The platanus trees, commonly known as the French sycamore, plays the most critical role in regulating the campus environment due to their tall trunks and dense canopies.



Figure 2. SEU within China and Nanjing; location of case area and information on architectural heritage.

2.3. The Microclimate Experiment Setup

The meteorological data measured by the experiment have two parts—data from the weather station and data from four portable measurement points. The meteorological data used for model simulation input came from measurements at an on-campus weather station, which was installed on the roof of a seven-floor building (Qiangong Building, Longitude: 118.80, Latitude: 32.06) on the SEU campus (Xuanwu District, Nanjing, Jiangsu Province). The weather station, presented in Figure 3, was from the Onset Computer Corporation. The measured data can be stored both offline and on an online server via a Wi-Fi channel. The simulation input data used in this study include air temperature (°C), relative humidity (%), dew point (°C), air pressure (mbar), rain (mm), solar radiation (W/m²), wind direction (°), and wind speed (m/s). Table 1 summarizes the basic information of the selected sensors concerning device version, operating temperature, accuracy, resolution, measurement range, and size.

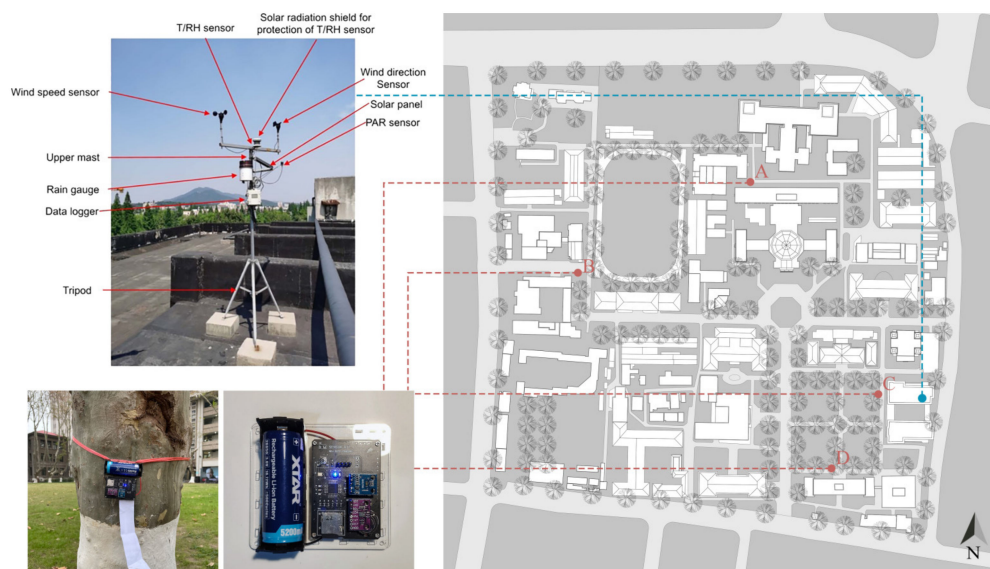


Figure 3. Location of SEU weather station, schematic map of measurement points, and photos of sensors.

Table 1. Basic information for sensors on the microclimate station.

	Data Logger	Temperature/Humidity	Wind Speed	Wind Direction	Solar Radiation
Version	RX3003	S-THB-M002	S-WSB-M003	S-WDB-M003	S-LIB-M003
Operating temperature	40–+60 °C	−40–+75 °C	−40–+75 °C	−40–+70 °C	−40–+75 °C
Accuracy	-	T: ±0.21 °C RH: ±2.5%	±1.1 m/s or ±4%	±5°	±10 W/m ² or ±5%
Resolution	-	T: 0.02 °C RH: 0.1%	0.5 m/s	1.4°	1.25 W/m ²
Measurement range	-	T: −40–+75 °C RH: 0–100%	0–76 m/s	0–355°	0–1280 W/m ²
Size (mm)	186(H) × 181(L) × 118(W)	10 × 35	410 × 16	460 × 200	41(H) × 32(Φ)

Four portable measurement points were in the study area (see Figure 3). The data from the four mobile measuring points were obtained by the sensors, which were fixed on-campus installations at a height of about 1.2 m that measured meteorological data (e.g., temperature, humidity, and wind speed). Table 2 summarizes the basic information for sensors on the portable measurement points. These data were acquired during a two-month measurement campaign (from 1 November 2020 to 31 December 2020) and used to validate the tree model using the measured data for 15 December 2020.

Table 2. Basic information for sensors on the portable measurement points.

Environment Data	Sensor Model	Precision	Range	Resolution
Temperature	DHT22	<±0.5 °C	−40–80 °C	0.1 °C
Humidity		±2% RH	20–90% RH	1% RH
Light intensity	BH1750FVI	1 lx	1–65535 lx	1 lx
CO ₂ concentration	CCS811	1 ppm	400–29,206 ppm	1 ppm
TVOC concentration		1 ppb	0–32,768 ppb	1 ppb

2.4. Simulation Model in ENVI-Met 4.4.6

ENVI-met 4.4.6 is a well-known microclimate model for simulating micro-urban areas. As a powerful simulation tool for viewing a range of urban environmental quality and outdoor thermal comfort criteria, this software comprehensively considers buildings, solar radiation, wind, green space, and many other factors [49]. We used ENVI-met in this study because it is based on a holistic 3D nonhydrostatic microclimate model that can realistically simulate climatic processes (e.g., the interaction between soil, atmosphere, and plants) in an urban environment with a typical resolution of 0.5 to 10 m in space and 10 s in time. Additionally, the BIO-met section of the software could further analyze urban thermal comfort using the results of the microclimate simulation [14].

Simulation using ENVI-met requires two initial files: (1) a model file including the location of buildings, vegetation, soil, surfaces, and receptors; and (2) a climate file containing all initial weather data (e.g., air temperature, relative humidity, solar radiation, precipitation, wind speed, and wind direction) and simulation time. A grid resolution of 5 m × 5 m × 4 m was used to digitize the campus area in the software to form a total area of 120 × 120 × 35 grids, equivalent to an area of 600 m × 600 m. Figure 4 shows the 3D bird's eye view of the models.

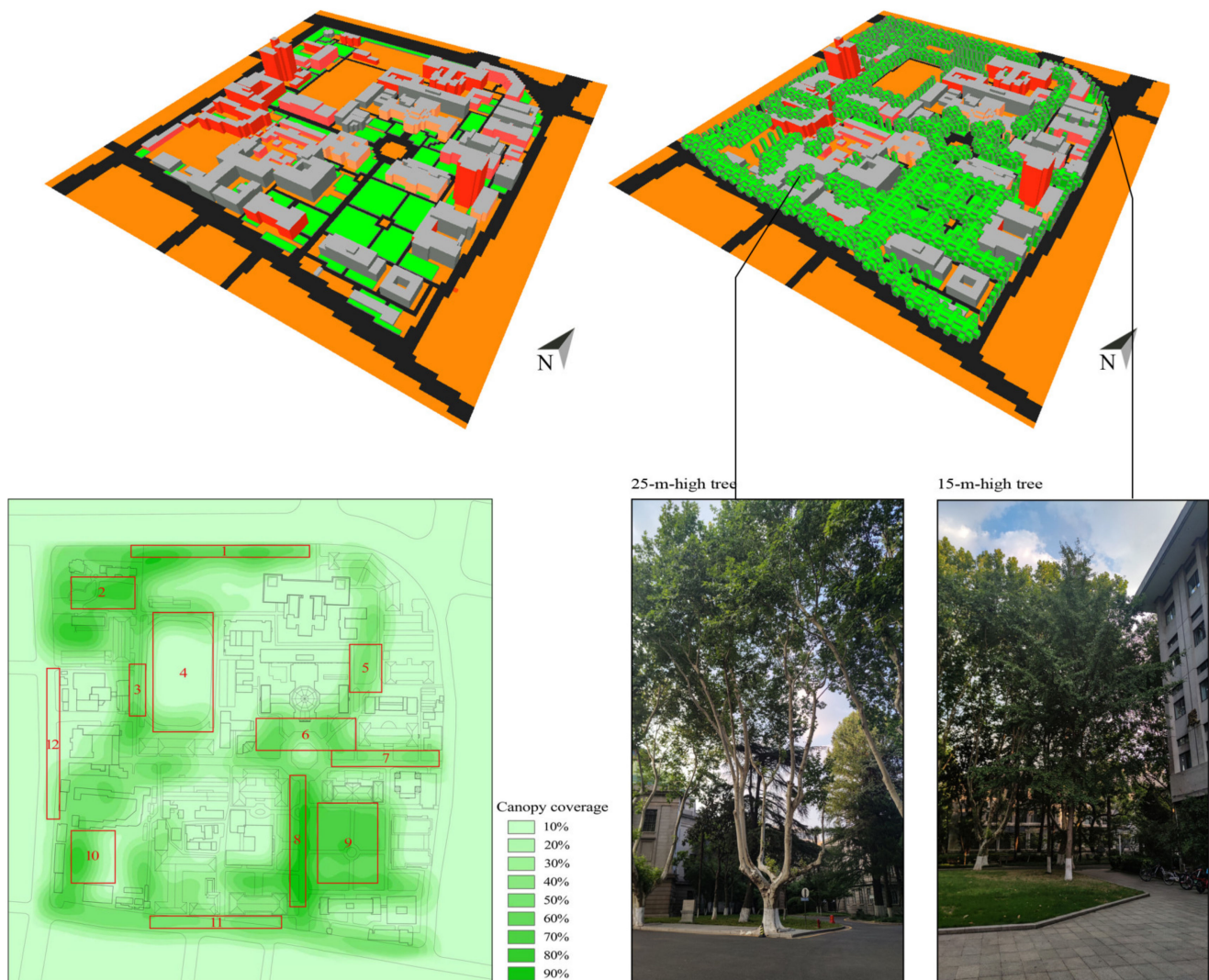


Figure 4. 3D bird's eye view of two control models and specific information for 12 blocks.

Through a full investigation and consideration of the actual site environment, we selected suitable materials to represent the building materials on campus (see Table 3). For all building roofs, moderate insulation was used. Four materials were chosen to represent building walls: (1) concrete wall of cast dense, (2) aerated brick wall, (3) burned brick wall, and (4) reinforced brick wall. Additionally, the vegetation selected in the model database could accurately represent real campus environment (see Table 4 for all vegetation parameters). First, we selected 50 cm of vegetation to represent the grassland. In addition, trees with a 25-m-high dense canopy and large trunks were used to represent the sycamores on campus. Small and medium-sized trees were represented by 15 m trees. The growth of trees as living organisms, however, is complex and diverse, and multiple species of trees are present on campus. The individual conditions of each species vary accordingly. Therefore, we could not fully model the species and shapes of trees. For the operability of the research, we divided the trees on campus into two categories according to height and canopy size and used the above two abstract trees to represent campus trees for specific studies. Finally, the surface parameters are presented in Table 5. Loamy soil was used to represent soil surface, and asphalt was used for streets.

Table 3. Selected physical properties of the building materials.

Materials	ID	Reflection	Emissivity	Specific Heat [J/(kg K)]	Thermal Conductivity [W/(mK)]
Moderate insulation	000000	0.50	0.90	850	1.60
Concrete wall (cast dense)	0000C5	0.30	0.90	840	1.90
Brick wall (aerated)	0000B1	0.40	0.90	840	0.30
Brick wall (burned)	0000B2	0.40	0.90	650	0.44
Brick wall (reinforced)	0000B3	0.40	0.90	840	1.10

Table 4. Selected physical properties of vegetation (LAD = leaf area density).

Vegetation	ID	Albedo	LAD
50 cm grass	0000XX	0.20	0.30
25 m trees	01HLDL	0.18	0.30
15 m trees	0000SK	0.20	0.30

Table 5. Selected physical properties of surface.

Surface	ID	Albedo	Emissivity
Loamy soil	000000	0.00	0.98
Asphalt road	0000ST	0.20	0.90

Data used after simulation and for validation were at the level of 1.2 m. PMV was calculated for a 35-year-old person (male) with a height of 1.75 m, a weight of 75 kg, a metabolic rate of 1.48 met (activity: walking at 1.21 m/s, surface area: 1.91 m²). The clothing level of 15 March and 15 September were both set as 0.7 clo. The parameters for 15 June and 15 December were set as 0.5 clo and 0.9 clo, respectively. The data visualization was carried out with LEONARDO, the functional module for data visualization and performance analysis of ENVI-met. In addition to the complex full-campus model, this study also established a control model without trees. Therefore, we named the two models as the tree model and treeless model. The simulation was programmed to run from 9:00 a.m. to 6:00 p.m., fully considering how trees impact the microclimate and comfort under sufficient solar radiation conditions. Four typical days—the 15 of March, June, September, and December—were chosen to represent the four seasons. The simulation results of the tree model in winter were compared with the actual measurement data to calibrate the model. Eventually, 12 small blocks using marquees were selected and analyzed to explore how trees impact the microclimate and comfort specifically. Figure 4 also shows the location and numbering of the 12 blocks (The numbers in the figure represent the box numbers), with tree canopy coverage across the campus clearly expressed.

2.5. Model Calibration Assessment

For model calibration, field measurements of air or surface temperatures should be compared to simulation results when ENVI-met is used, as suggested by the conclusions of other researchers [50]. Calibration was performed in this study by comparing the actual temperature at four measurement points and the simulated temperature at the corresponding monitoring points in the simulation model on 15 December 2020. The final validation process only used air temperature because it is a highly descriptive and stable parameter that can be collected. Other parameters (e.g., wind speed and solar radiation) are sensitive to large changes easily affected by special factors. Evaluation indicators based on model prediction error include mean absolute error (MAE), mean bias error (MBE), mean absolute percentage error (MAPE), and root mean square error (RMSE). Two indicators,

RMSE and MAPE, were used as the standard for evaluating the simulation results, as shown in the equations below.

$$RMSE = \sqrt{\frac{\sum_{i=1}^n (y'_i - y_i)^2}{n}} \tag{1}$$

$$MAPE = \frac{1}{n} \sum_{i=1}^n \frac{|y'_i - y_i|}{y_i} \times 100\% \tag{2}$$

where, y'_i represents the simulated value, y_i represents the measured value, and n represents the number of actual measurements.

3. Results

3.1. Validation Results of Simulation Model in ENVI-Met

Figure 5 shows the distribution of simulated and measured air temperature at four points. The measured temperature values are clearly higher than simulated values at point A, while measured temperature values are mostly lower than simulated values at point D, which may be caused by measurement errors. However, the measured and simulated data are generally in good agreement because most differences between them in Figure 5 are stable at about 1 °C. Table 6 shows the evaluation indicators based on model prediction error. The MAPE figures of four points are all below 20%, suggesting that measured and simulated data can be well-fitted. Meanwhile, the gap between the measured and simulated data is acceptable because RMSE figures are mostly less than 1. To summarize, the validation assessment shows overall good results, and the trees model has good reliability.

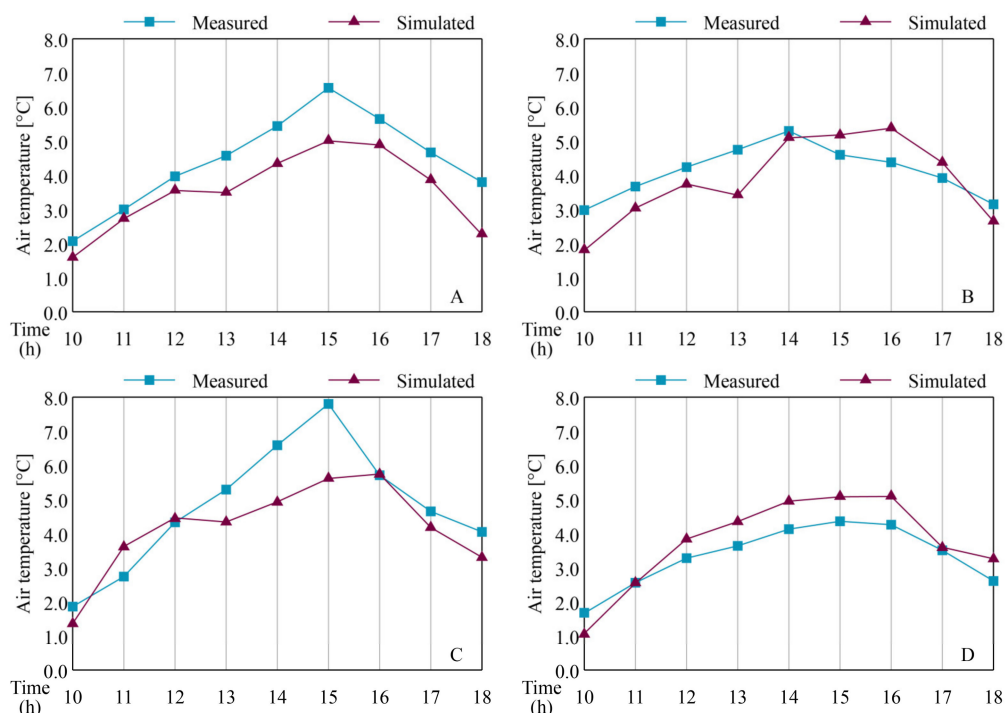


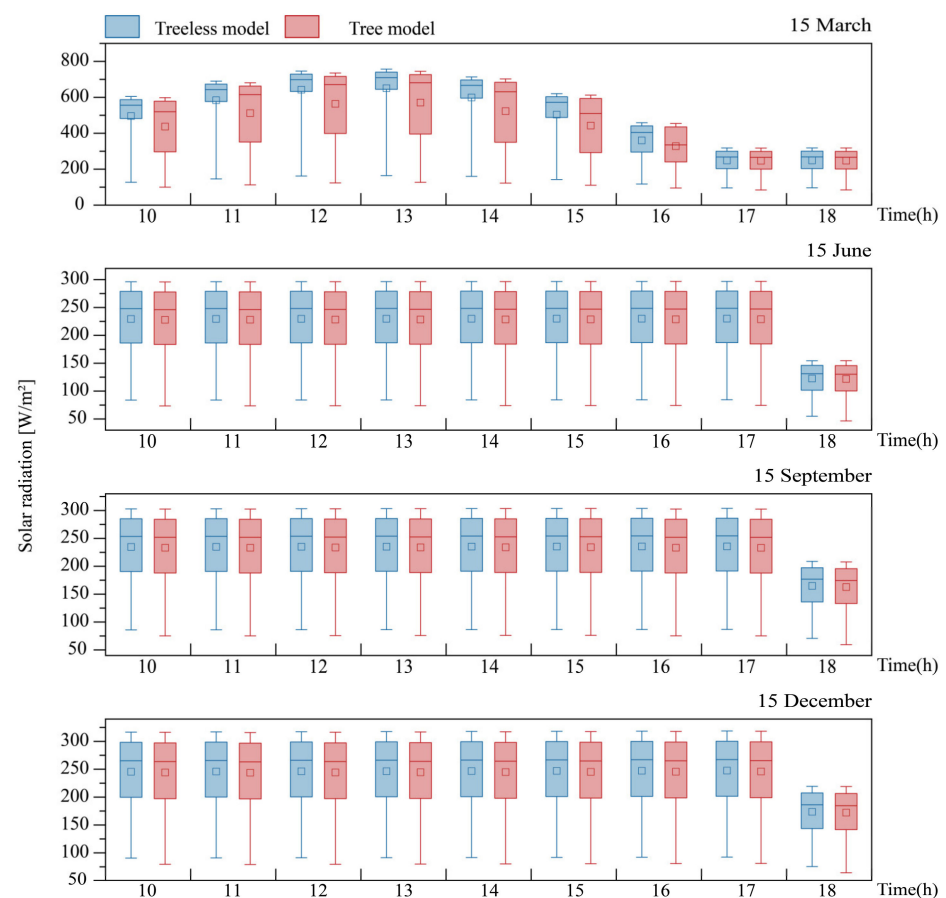
Figure 5. Simulated and measured air temperature at four portable measurement points.

Table 6. Calibration results of temperature at four monitoring points.

Sensor Point	MAPE	MSE	RMSE (°C)
A	18.6%	0.88	0.94
B	17.5%	0.60	0.77
C	17.5%	1.08	1.04
D	18.6%	0.44	0.67
Average	18.05%	0.75	0.855

3.2. Results of Solar Radiation Distribution

The simulated solar radiation results include direct, diffuse, and reflected solar radiation. According to information from the weather station, only 15 March was sunny. The other three days were cloudy. Therefore, during the daylight of 15 March, direct solar radiation was present but was not present on the other three days, on which only diffuse and reflected solar radiation was present. Based on the results for 15 March, the solar radiation of the tree model was significantly lower than that of the treeless model with the medians of data basically reduced by 100 W/m^2 (see Figure 6). The medians of data between two models were basically the same in the results for the 15 of June, September, and December, but the minimum values of the tree model were slightly lower by about 10 W/m^2 . Moreover, solar radiation values for 15 March fell in the range of 150 to 800 W/m^2 , putting them much higher than for the other three days (which ranged from 50 to 350 W/m^2). These results indicate that trees significantly impact the shading solar radiation when the sun is shining directly, but only limitedly impact solar radiation on cloudy days.

**Figure 6.** Comparison of the range of solar radiation between two models at a height of 1.2 m on four days.

3.3. Results of Air Temperature between Buildings

Based on simulated results of ENVI-met, the LEONARDO plug-in was applied in visualization for a clearer understanding how trees impact the air temperature between buildings. Figure 7 shows that, on 15 March, the medians of air temperature between two models were roughly close given the range of 14 to 21 °C. However, the data range in the tree model was larger, with higher maximum values and lower minimum values compared to the treeless model. On the 15 of June, September, and December, the air temperature of the tree model was obviously higher than that of the treeless model, with medians increasing by around 1 °C. The data range of tree model was also larger. Figure 8 shows comparative results between the two models for air temperature, wind speed, and PMV (values on cloud maps = tree model simulation minus treeless model simulation). Through an air temperature comparison between two models, we found that the temperature with trees decreases in some locations but increases in other locations compared with the treeless model. Results for 15 March indicated small differences in the magnitude of temperature increases and decreases. Results for the other three days showed that temperature at some campus locations increased the most (2.3 °C on average), but lowered positions decreased the most (0.18 °C on average). It is also common for locations with lower temperatures to be mostly at the edge of the building group and those with higher temperatures to be mostly in the interior. Therefore, these results indicate that different effects of trees on air temperature may be related to not only direct sun exposure, but also how and where trees are laid out.

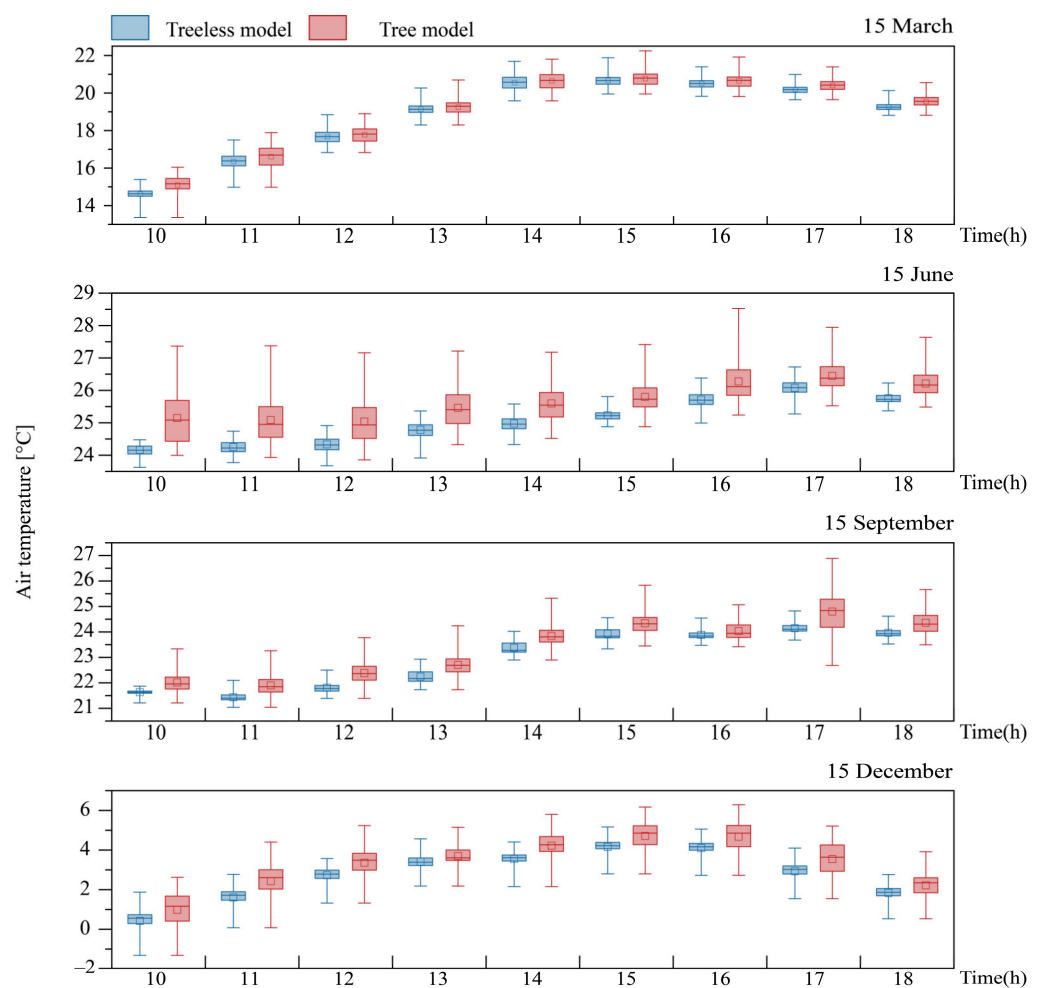


Figure 7. Comparison of the range of air temperature between two models at a height of 1.2 m on four days.

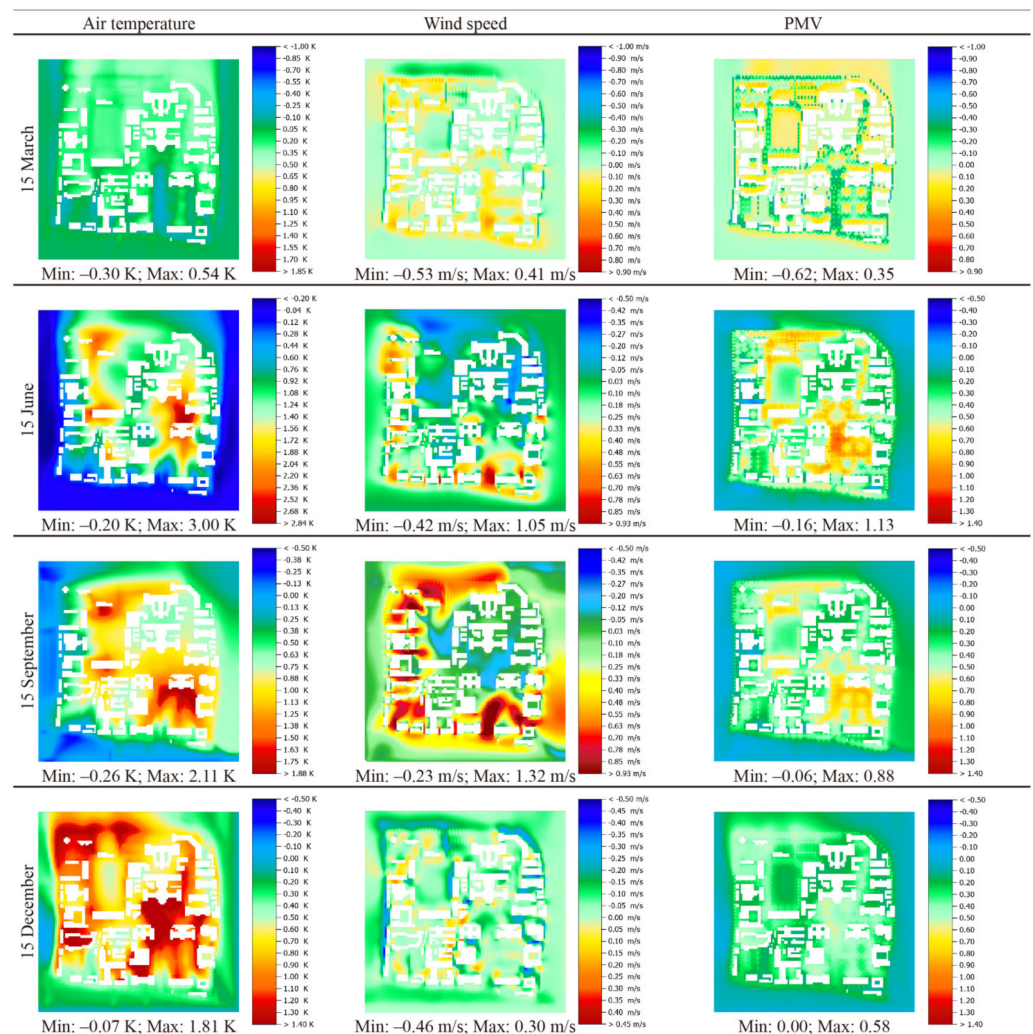


Figure 8. Comparative cloud maps of air temperature, wind speed, and PMV at a height of 1.2 m at 12:00 p.m. on four days. (Comparative results = Tree model simulation minus treeless model simulation).

3.4. Results of Wind between Buildings

The boxplots of Figure 9 show that the variation trend of wind speed. Results for 15 March and December indicated that median wind speeds between the two models were basically close but that the numerical range was larger in the tree model. Results for the other two days showed that the maximum wind speed values of increased significantly, with many growing more than 1 m/s. The cloud maps in Figure 8 show that wind speed decreased in some campus locations but increased in other areas with trees present. The 15 June and September results showed that wind speed increased significantly at some locations, as much as 1.18 m/s, on average. Additionally, from the distribution of cloud maps, the positions with increased wind speed were generally at the edge of the building complex, especially with trees on the windward side in a determinant distribution along the road. Wind speed inside the building complex, however, was generally reduced with enclosed or aggregated trees. In sum, the results above indicate that the trees caused two types of airflow changes, which can be strengthened or weakened. The specific airflow changes could be related to the season, tree layout, and location.

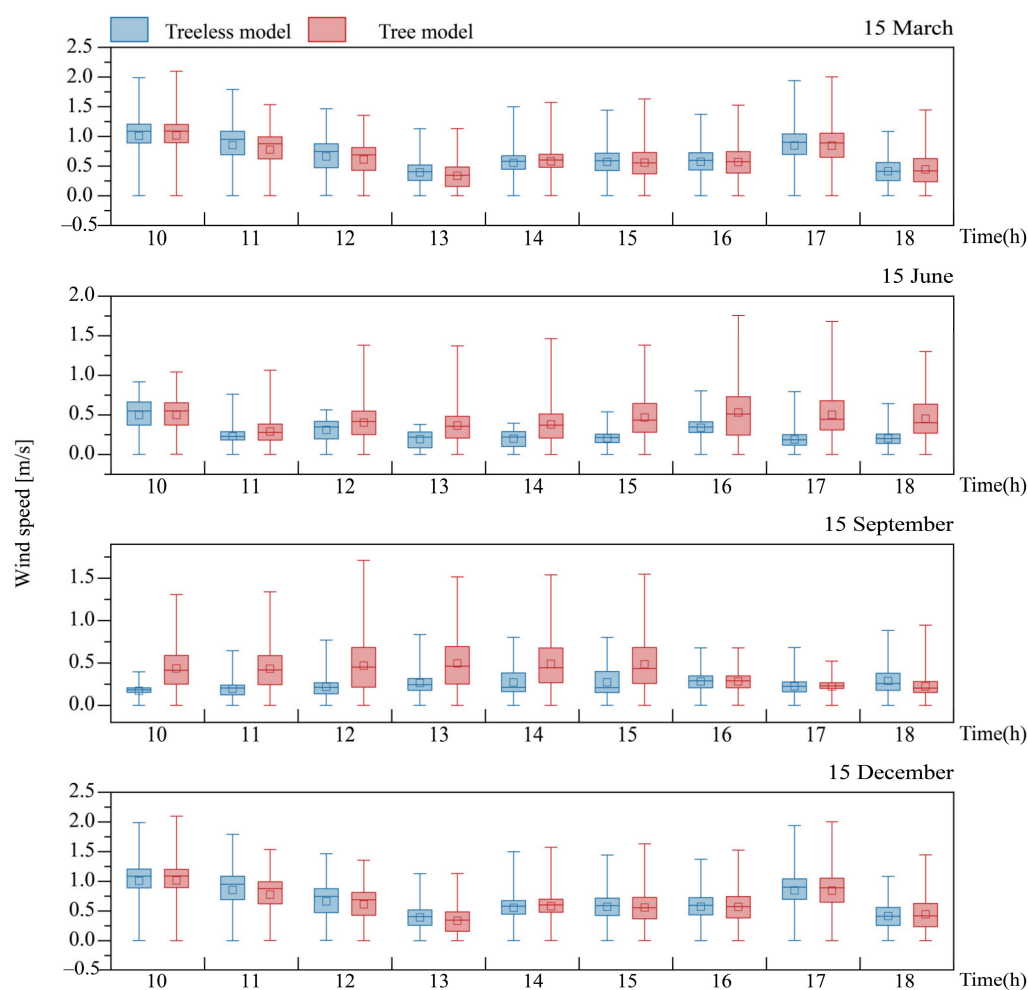


Figure 9. Comparison of the range of wind speed between two models at a height of 1.2 m on four days.

3.5. Results of Outdoor Thermal Comfort (PMV) between Buildings

To obtain the thermal comfort, we imported atmosphere data from the first simulation into BIO-met and recalculated. Figure 10 shows that the medians for 15 March between the two models were basically close, but the data range of tree model was larger. Results for the other three days indicate that the PMV of the tree model was higher than that of the treeless model, with medians increasing about 0.2 and maximum values increasing about 0.5. In Figure 8, the cloud maps show that, on 15 March, PMV exhibited a decreasing trend in some locations and an increasing one in other locations with trees present. The locations with reduced PMV are basically nodes where green plants are denser given that trees distributed in a determinant pattern decreased by at most 0.62. Results for the other three days indicate that PMV values basically increased throughout the map, with outdoor space surrounded by trees increasing the most.

As is well-known, the higher the PMV values, the warmer human bodies feel outdoors, and the lower the values, the colder human bodies feel. The results above imply that the impacts of trees on outdoor thermal comfort are relatively complex. Trees on campus may affect thermal comfort by transpiration, shading radiation, and changing airflow, but the impacts are related to season, direct sun exposure, tree layout, and location. More specifically, our results showed that trees led to lower PMV on 15 March with direct sunlight. This finding means that, on sunny days, dense greenery could greatly improve outdoor thermal comfort [51,52]. Results on the other three days showed that the thermal comfort of human bodies could be significantly improved by trees blocking wind on cold days and

that, in summer days without direct sunlight, trees can also make people feel hotter than they would in locations without trees.

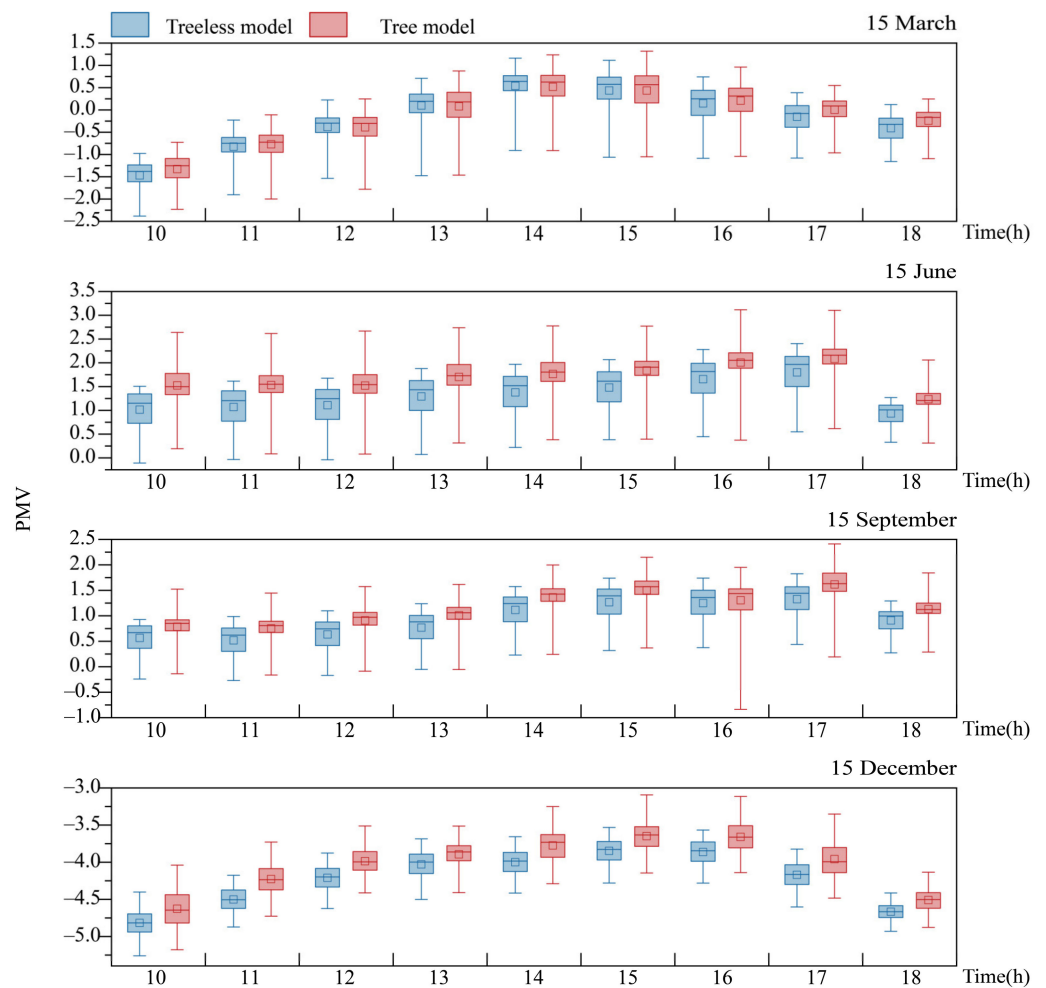


Figure 10. Comparison of the range of PMV between two models at a height of 1.2 m on four days.

3.6. Results of Façade Temperature

Based on the actual simulated results (see Figure 11), urban trees seemingly impact buildings' façade temperatures. Results for 15 March indicate that the façade temperature of the building's south, partial west, and east in the tree model revealed a clear downward trend with a maximum of 8.73 °C. The same results also showed that, the lower the number of floors, the more the façade temperature dropped. Results for the other three days illustrated that most of the buildings' façade temperatures revealed an upward trend in the tree model, increasing the most 8.48 °C on average. However, several high-rise buildings demonstrated another interesting phenomenon—the façade temperature dropped significantly above a certain height. Based on the results above, we believe trees also have multiple impacts—which are related to direct sun exposure, tree layout, and location—on the façade temperature. Based on the results for 15 March, when the sun shines directly, trees can shelter solar radiation, reduce heat gained, and eventually decrease the façade temperature on the sunny side of buildings. Additionally, trees could also change airflow and wind speed, thereby affecting façade temperature. Based on the results for the other three days, the elevated façade temperature indicates that the wind-blocking effect of trees is dominant at this time. The special phenomenon exhibited by high-rise buildings further confirms how trees affect airflow (see Figure 12). As a result of trees blocking, airflow was more concentrated on the upper layer of trees, which increased wind speed

there. That cause the façade temperature above this height to drop significantly, while the façade temperature below this height continued rising.

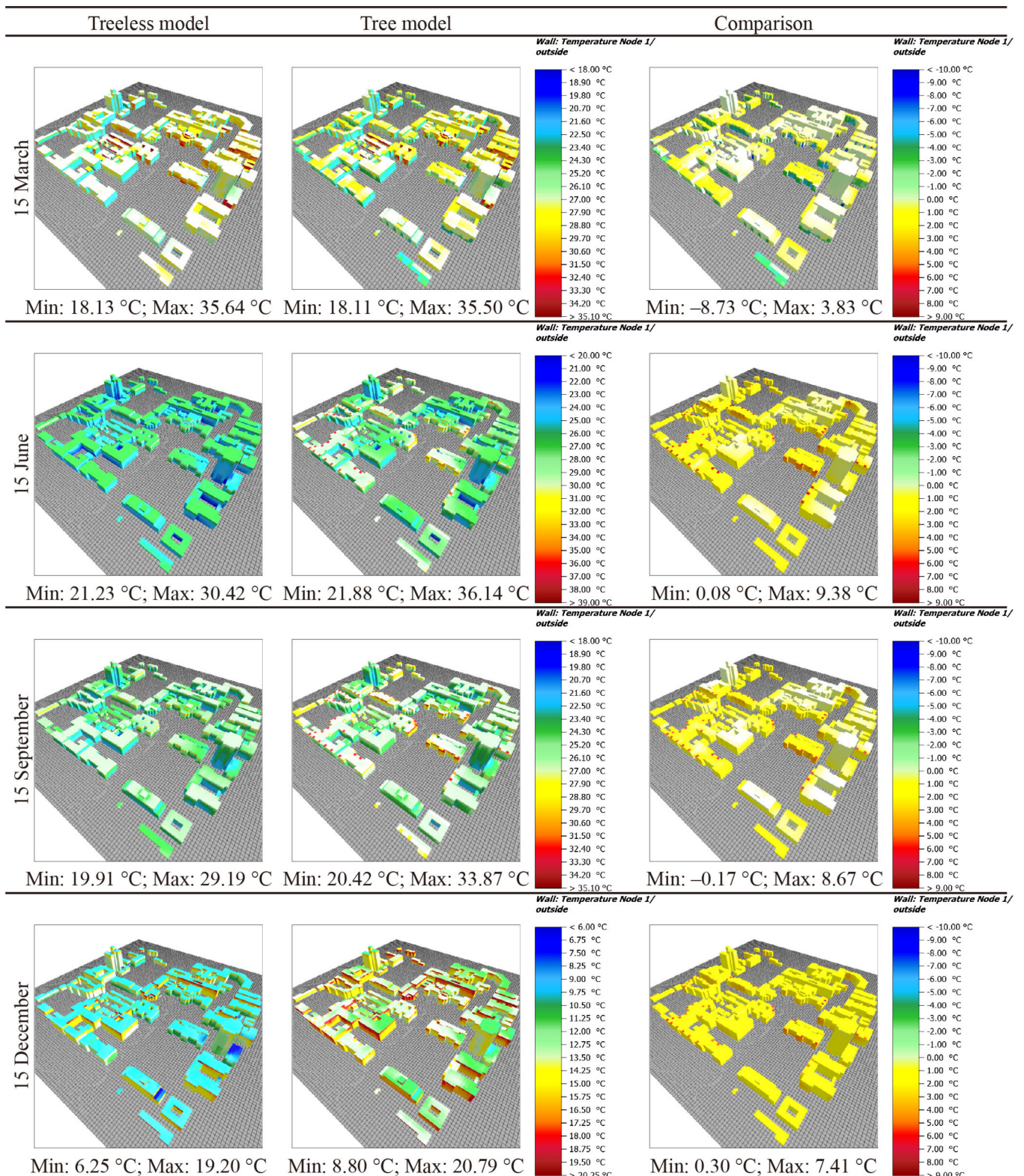


Figure 11. Distribution of simulated façade temperature at 12:00 p.m. on four days. (Comparison = Tree model simulation minus treeless model simulation).

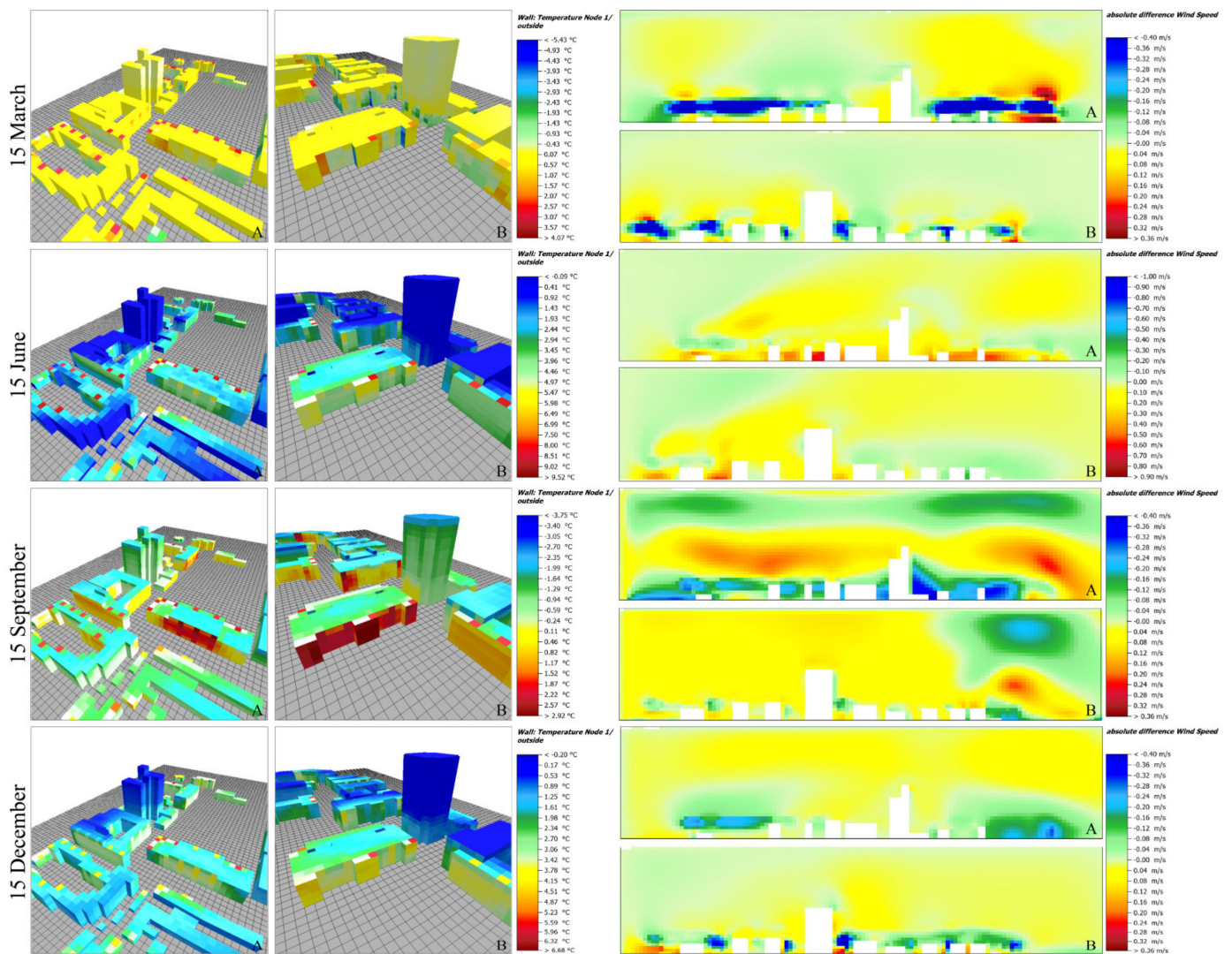


Figure 12. Façade temperature and surrounding airflow changes of two high-rise buildings at 16:00 p.m. on four days.

3.7. Results of Overall Average Comparison

As shown in Figure 13, the variation in the microclimate and comfort is clearly related to season and the presence of direct sunlight. For 15 March, a sunny day, solar radiation dropped significantly, with a maximum variation of 80 W/m^2 . For the other three cloudy days, solar radiation decreased very little, and the variation basically did not exceed 3 W/m^2 . The variation in air temperature and PMV was generally positively correlated. Further, the increasing values for air temperature and PMV on 15 March were relatively small, not exceeding $0.5 \text{ }^\circ\text{C}$ and 0.15, respectively. For wind speed variation, a certain decrease occurred on 15 December with a change of up to 0.08 m/s , and some increases occurred on 15 June and 15 September. On those two dates, the amount of wind speed variation clearly exhibited a negative correlation with that of air temperature variation. In sum, the results above show that, for 15 March, the shading effect of trees on solar radiation was dominant due to direct sunlight, but for 15 June and 15 September, the effect of trees on airflow was dominant. Additionally, for 15 December, air temperature increased significantly when wind speed decreased partially due to low winter temperatures.

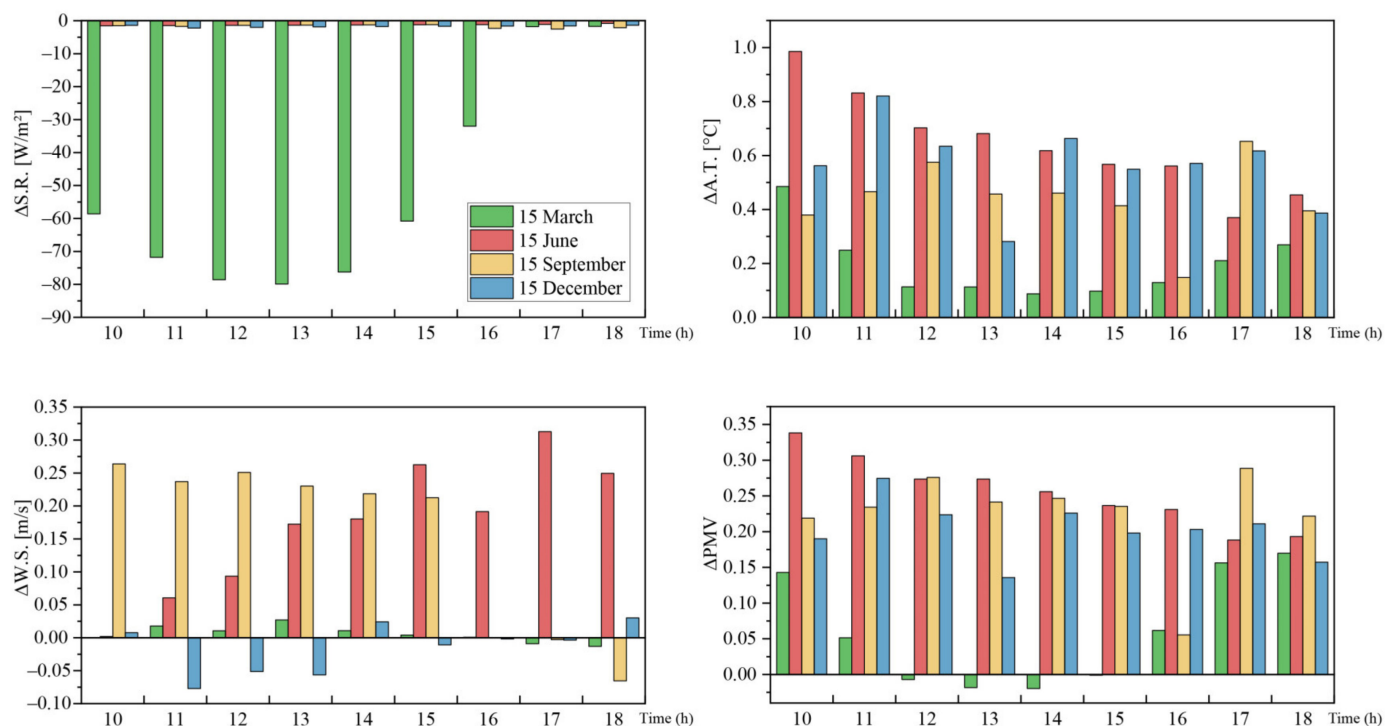


Figure 13. Average comparison in the microclimate and comfort between two models at a height of 1.2 m on four days. (Comparison (Δ) = Tree model simulation minus treeless model simulation; S.R. = solar radiation; A.T. = air temperature; W.S. = wind speed).

3.8. Results of Marquee Data

Based on the simulated results and blocks delineated, we counted the average comparison differences (comparison (Δ) = tree model minus treeless model) in the microclimate and comfort for 12 blocks at 12:00 p.m. on four days and recorded canopy coverage, layout, and location (listed in Appendix A, Table A1). Figure 14 shows the comparison between 12 blocks on 15 March (y -axis: ΔPMV , x -axis: $\Delta S.R.$) and 15 December (y -axis: $\Delta A.T.$, x -axis: $\Delta W.S.$) with bubble plots. For 15 March, the average compared solar radiation values were basically negative, and the PMV values decreased. In addition, the marquee with the most canopy coverage of 97% had the largest reduction in mean solar radiation and PMV of $-288.7 W/m^2$ and -0.23 , respectively. Based on the results above, trees impact comfort by sheltering solar radiation on sunny days with direct solar radiation. Generally, the larger the canopy coverage, the greater the reduction in solar radiation and the lower the PMV. For 15 December, average comparison wind speed values were mostly negative, and air temperature increased. The marquee with canopy coverage of 41.5% whose layout is enclosed inside the complex, had an average reduction in wind speed of $0.03865 m/s$ and the largest increase in air temperature ($1.4 ^{\circ}C$). However, canopy coverage had little impact on how much wind speed was reduced at that time. Therefore, trees impact the microclimate through the wind-blocking effect on airflow during the winter and its low temperatures, especially for trees enclosed in the building group.

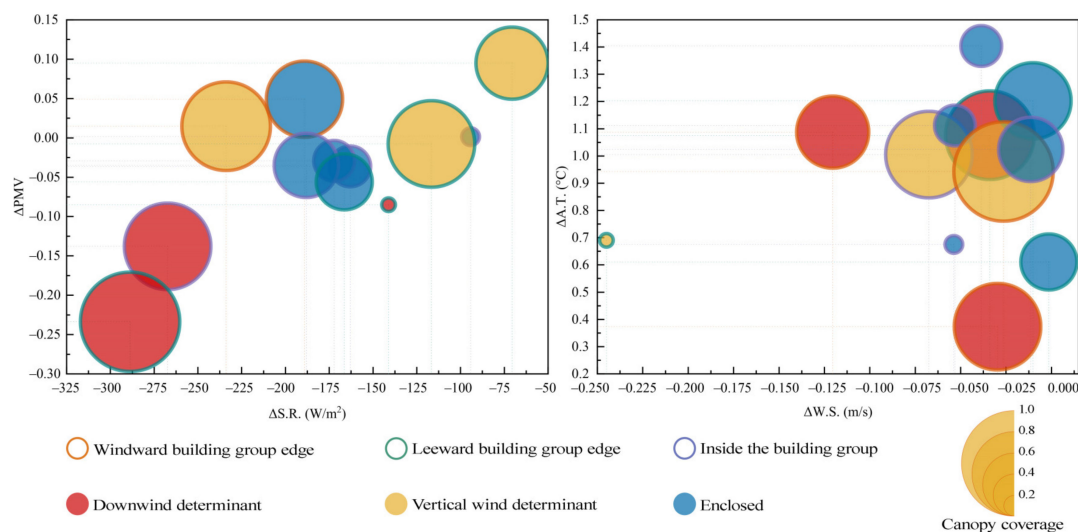


Figure 14. Bubble diagrams of 12 marquees on 15 March (left) and 15 December (right).

4. Discussion

In this study, a campus area was selected as the case to explore multiple impacts of trees on improving urban environment and examined the consequences of these impacts. Further, based on the above results, we explored when these impacts were dominant and their relationship to season, direct sun exposure, tree layout, and location. On sunny days with direct sunlight, the sheltering and transpiration effects of trees dominated, contributing to the lower temperature and improving comfort around trees. The tree species' impact on airflow played a major role on cloudy days without direct sunlight. At the edge of the windward building group, street trees following the wind direction produced the wind channel effect, strengthening airflow, increasing wind speed, and reducing air temperature. Meanwhile, street trees in the vertical wind direction did not change much. Enclosed trees inside the building group had the wind-blocking effect, weakening airflow, decreasing wind speed, and increasing air temperature. For the façade temperature, on sunny days, trees sheltered solar radiation to decrease the temperature of building sunny side. On cloudy days, trees mainly weakened the airflow due to the wind-blocking effect, and the façade temperature of the whole building complex somewhat increased. Moreover, high-rise buildings on the upper layer of trees caused the wind speed to increase and the façade temperature to decrease due to the accumulation of airflow. Of course, the two trees selected for this study had differential effects in terms of shading and airflow. The first effect is that the two trees naturally differ in their ability to shade solar radiation due to having different sized canopies. For the simulation results of 15 March (see Figure 10), a 25-m-high tree had a larger area, with PMV decreasing around it due to the larger canopy. Secondly, the difference in height of the two trees caused them to affect airflow differently. Based on the analysis of the trees around the high-rise building, 15-m-high trees are less effective in blocking the airflow than 25-m-high trees.

This study clarified that the improvement of the microclimate by having urban trees will affect the building's façade temperature, which obviously varies alongside the influence of urban trees. On one hand, optimizing the microclimate can therefore also influence the indoor environment via interaction with the outdoor environment through building facades and undoubtedly further impact both the heat transfer of building exterior walls and building energy consumption. Another issue worthy of further research on green urban design is how to optimize tree or urban greening while maintaining a balance between reducing building energy consumption and improving outdoor thermal comfort. On the other hand, several architectural heritages are present within our study area, and their conservation is very important. This study has great value for studying how vegetation can play a role in the conservation of architectural heritages and change the life of exterior

walls (slowing or accelerating the rate of building aging). In addition, tree canopies have important shading functions for the buildings, so how to calculate, map, measure, simulate, and evaluate the specific contribution of trees is an important task. By altering the microclimate around the building, trees add a buffer between the buildings and the external environment. In the future, we will focus on how to quantify this invisible buffer zone and relate it to the parameters of trees and canopies, leading to more specific and quantifiable conclusions.

Importantly, this study has some limitations. One is model validation—this study selected the measured data in the winter for calibration, but the more rigorous approach would be to increase the comparison in the summer to achieve a more critical validation process. On the other hand, this study selected four evenly distributed sensor monitoring spots for the validation. Testing at the actual monitoring spots should be required in future studies to ensure a more scientific validation. Secondly, when analyzing the simulated results of the façade temperature, a more detailed and comprehensive comparison should be conducted. Due to being limited to the software version used, this study did not numerically analyze the façade temperature with full statistics, resulting in no comparison among the four materials used in the building envelope. Thirdly, since running the microclimate simulation in ENVI-met was time consuming, only four typical days were selected to simulate different seasons. The potential approach would be to select an equal number of sunny and cloudy days in each season for simulation and comparison. In the future, more simulation cases should be added, and some new simulation methods should be applied to speed up the simulation process and test the results in more days and scenarios. Finally, this study focuses on a campus case, with trees, buildings and building materials, and substrate materials set based on the current campus environment. Our findings can therefore be used to optimize the campus building group design. More sustainable and comfort public space through urban design should be enriched, and the city is also usually complex and full of favored areas with a pleasant microclimate as well as disfavored areas that need improving. In the future, our work will focus on more complex urban situations and environments, and we will study microclimates with more diverse trees and materials to obtain more accurate and generalized conclusions. Incidentally, the literature review in this paper analyzed previous explorations of the relationship between urban morphology and microclimate. In the future, we can quantify urban morphology indicators and explore the correlation between morphology and microclimate, then focus on optimizing urban design for the pre- and post-design evaluation by integrating the effects of both urban morphology and trees.

5. Conclusions

This study elucidated how urban trees can influence the microclimate, thermal comfort, and building façade temperature via comparing a trees model with a treeless model. Results showed that trees impact microclimate and thermal comfort in at least three ways. Firstly, the transpiration of vegetation itself can reduce the air temperature and improve thermal comfort. Secondly, trees can shelter solar radiation, reduce heat accumulation, and decrease air temperature by at most 0.3 °C, especially on sunny days. PMV on sunny days could also be decreased by at most 0.62 due to shade from trees. The other two impacts are mainly related to how trees impact airflow. At the edge of the building group, trees arranged in a determinant following the wind direction can produce the wind channel effect, which could increase wind speed by at most 1.32 m/s and decrease air temperature by at most 0.26 °C. Enclosed trees inside the building group, however, could cause the wind-blocking effect, which decreases wind speed by at most 0.53 m/s and increases PMV by at most 1.13. Further, how trees impact the façade temperature mainly manifests as sheltering solar radiation and blocking airflow. Shading solar radiation is the dominant impact on sunny days with façade temperature decreasing by at most 8.73 °C. Meanwhile, blocking wind is dominant on cloudy days, with the façade temperature increasing by at most 9.38 °C. For

high-rise buildings, strengthened airflow on the upper layer of trees could decrease the façade temperature there by up to 3.75 °C.

Based on the overall comparison results, the impacts of trees are related to season and direct sun exposure. On sunny days with direct sunlight, the sheltering effect on solar radiation is dominate, with an average reduction in solar radiation of up to 80 W/m² and an average reduction in PMV of up to 0.02. Conversely, the effects of trees on airflow are dominate on cloudy days. Trees have both wind channel and wind-blocking effects during summer and autumn, but only a wind-blocking effect in winter. To further investigate the detailed role of trees, 12 small blocks were selected with the attributes of canopy cover, layout, and location, with comparison values of the microclimate and comfort tallied. The results indicate that high canopy coverage facilitates the sheltering effect on solar radiation and that the effect of trees on airflow is closely related to layout and location. Enclosed trees inside the building group often exert a wind-blocking effect, decreasing wind speed and increasing air temperature, while downwind determinant trees located windward at the building group edge are more likely to exert the wind channel effect, increasing wind speed and decreasing air temperature. Therefore, these findings provide important reference for green urban design and landscape design.

Author Contributions: Conceptualization, L.D. and W.W.; methodology, L.D.; software, L.D. and X.J.; validation, L.D., X.J. and W.W.; formal analysis, W.W.; investigation, L.D. and X.J.; data curation, L.D.; writing—original draft preparation, L.D. and W.W.; writing—review and editing, S.A.H.; visualization, L.D. and X.J.; supervision, W.W. and S.A.H.; project administration, W.W.; funding acquisition, W.W. All authors have read and agreed to the published version of the manuscript.

Funding: The work described in this paper was sponsored by National Key R&D Program of China (NO. 2019YFD1100903). Any opinions, findings, conclusions, or recommendations expressed in this paper are those of the authors and do not necessarily reflect the views of those organizations.

Conflicts of Interest: The authors declare no conflict of interest.

Appendix A

Table A1. Average comparison values in microclimate and comfort for the 12 marquees on four days. (Layout: DD = downwind determinant; VWD = vertical wind determinant; E = enclosed. Location: WBGE = windward building group edge; LBGE = leeward building group edge; IBG = inside the building group).

(a). 15 March							
	Canopy Coverage	Layout	Location	$\Delta S.R.$ (W/m ²)	$\Delta A.T.$ (°C)	$\Delta W.S.$ (m/s)	ΔPMV
1	0.866667	VWD	WBGE	−233.884	0.295177	0.118485	0.014867
2	0.75	E	WBGE	−189.122	0.274677	0.108939	0.049034
3	0.846154	DD	IBG	−267.35	0.204117	0.009501	−0.13796
4	0.2	E	IBG	−94.313	0.187346	0.024717	0.001508
5	0.416667	E	IBG	−163.057	0.300329	−0.02448	−0.03615
6	0.415	E	IBG	−172.207	0.14311	0.050275	−0.02917
7	0.712963	VWD	LBGE	−70.6579	0.24253	0.009321	0.095042
8	0.969697	DD	LBGE	−288.685	−0.16867	0.232768	−0.23363
9	0.636667	E	IBG	−188.129	0.051496	0.088151	−0.03499
10	0.559441	E	LBGE	−166.405	−0.02918	0.0913	−0.05598
11	0.848485	VWD	LBGE	−116.632	0.015353	0.085779	−0.0078
12	0.157895	DD	LBGE	−141.165	0.016937	−0.17098	−0.08489

Wind direction: 12°

Table A1. Cont.

(b). 15 June							
	Canopy Coverage	Layout	Location	$\Delta S.R.$ (W/m ²)	$\Delta A.T.$ (°C)	$\Delta W.S.$ (m/s)	ΔPMV
1	0.866667	VWD	LBGE	−1.44717	1.607159	−0.13122	0.663578
2	0.75	E	LBGE	−1.03549	1.444576	0.368378	0.61605
3	0.846154	DD	IBG	−1.76956	1.574533	−0.04317	0.604991
4	0.2	E	IBG	−1.33	1.319982	−0.03592	0.440936
5	0.416667	E	IBG	−2.44453	1.724289	−0.17888	0.582411
6	0.415	E	IBG	−2.44318	1.913297	0.031413	0.656675
7	0.712963	VWD	WBGE	−2.68608	1.894526	0.131189	0.64751
8	0.969697	DD	WBGE	−1.68921	1.089008	0.426054	0.54987
9	0.636667	E	IBG	−2.73334	1.53011	0.261862	0.612494
10	0.559441	E	WBGE	−1.21009	0.573616	0.24289	0.3408
11	0.848485	VWD	WBGE	−1.53628	0.196246	0.247588	0.259214
12	0.157895	DD	LBGE	−3.18532	0.016658	0.120382	0.120383
Wind direction: 156°							
(c). 15 September							
	Canopy Coverage	Layout	Location	$\Delta S.R.$ (W/m ²)	$\Delta A.T.$ (°C)	$\Delta W.S.$ (m/s)	ΔPMV
1	0.866667	DD	WBGE	−1.44088	0.891596	0.644554	0.464355
2	0.75	E	WBGE	−0.97823	0.628945	0.642251	0.399441
3	0.846154	VWD	IBG	−1.73729	0.743274	0.376512	0.384758
4	0.2	E	IBG	−1.32415	1.071369	0.418308	0.370467
5	0.416667	E	IBG	−2.44445	0.810564	−0.0664	0.353771
6	0.415	E	IBG	−2.45151	1.065336	−0.0966	0.439253
7	0.712963	DD	LBGE	−2.6319	1.175472	0.082519	0.466394
8	0.969697	VWD	LBGE	−1.65825	1.262547	0.599528	0.561655
9	0.636667	E	IBG	−2.68482	1.511156	0.536059	0.582903
10	0.559441	E	WBGE	−1.17841	0.488601	0.631484	0.298461
11	0.848485	DD	WBGE	−1.44598	0.458734	0.396177	0.291394
12	0.157895	VWD	WBGE	−3.2256	−0.02397	0.196467	0.08979
Wind direction: 267°							
(d). 15 December							
	Canopy Coverage	Layout	Location	$\Delta S.R.$ (W/m ²)	$\Delta A.T.$ (°C)	$\Delta W.S.$ (m/s)	ΔPMV
1	0.866667	DD	LBGE	−2.12521	1.076418	−0.03395	0.434424
2	0.75	E	LBGE	−1.41085	1.202791	−0.01014	0.458446
3	0.846154	VWD	IBG	−2.27264	1.005118	−0.06748	0.384099
4	0.2	E	IBG	−1.90624	0.675531	−0.05376	0.245573
5	0.416667	E	IBG	−3.11303	1.112071	−0.05318	0.377153
6	0.415	E	IBG	−3.14581	1.404079	−0.03865	0.464138
7	0.712963	DD	WBGE	−2.85953	1.087835	−0.12042	0.386298

Table A1. Cont.

	Canopy Coverage	Layout	Location	$\Delta S.R.$ (W/m ²)	$\Delta A.T.$ (°C)	$\Delta W.S.$ (m/s)	ΔPMV
8	0.969697	VWD	WBGE	−2.17563	0.942917	−0.02643	0.411017
9	0.636667	E	IBG	−2.77692	1.023979	−0.0114	0.397938
10	0.559441	E	LBGE	−1.7789	0.610644	−0.00148	0.273837
11	0.848485	DD	WBGE	−1.62501	0.373165	−0.02964	0.210405
12	0.157895	VWD	LBGE	−4.10567	0.690514	−0.245	0.232986

Wind direction: 129°

References

- National Bureau of Statistics of China. *Statistical Communiqué of the People's Republic of China on the 2021 National Economic and Social Development*; National Bureau of Statistics of China: Beijing, China, 2022.
- Chen, M.; Liu, W.; Lu, D. Challenges and the Way Forward in China's New-Type Urbanization. *Land Use Policy* **2016**, *55*, 334–339. [[CrossRef](#)]
- Wang, Q.; Wu, S.D.; Zeng, Y.E.; Wu, B.W. Exploring the Relationship between Urbanization, Energy Consumption, and CO₂ Emissions in Different Provinces of China. *Renew. Sustain. Energy Rev.* **2016**, *54*, 1563–1579. [[CrossRef](#)]
- Martinelli, L.; Lin, T.P.; Matzarakis, A. Assessment of the Influence of Daily Shadings Pattern on Human Thermal Comfort and Attendance in Rome during Summer Period. *Build. Environ.* **2015**, *92*, 30–38. [[CrossRef](#)]
- Lappen, C.-L.; Schumacher, C. Rapid urbanization and changes in spatiotemporal characteristics of precipitation in Beijing metropolitan area. *J. Geophys. Res.* **2014**, *119*, 2966–2989. [[CrossRef](#)]
- Hondula, D.M.; Georgescu, M.; Balling, R.C. Challenges Associated with Projecting Urbanization-Induced Heat-Related Mortality. *Sci. Total Environ.* **2014**, *490*, 538–544. [[CrossRef](#)]
- Kim, S.W.; Brown, R.D. Urban Heat Island (UHI) Intensity and Magnitude Estimations: A Systematic Literature Review. *Sci. Total Environ.* **2021**, *779*, 146389. [[CrossRef](#)]
- Tong, S.; Wong, N.H.; Tan, C.L.; Jusuf, S.K.; Ignatius, M.; Tan, E. Impact of Urban Morphology on Microclimate and Thermal Comfort in Northern China. *Sol. Energy* **2017**, *155*, 212–223. [[CrossRef](#)]
- Bowler, D.E.; Buyung-Ali, L.; Knight, T.M.; Pullin, A.S. Urban Greening to Cool Towns and Cities: A Systematic Review of the Empirical Evidence. *Landsc. Urban Plan.* **2010**, *97*, 147–155. [[CrossRef](#)]
- He, X.; Gao, W.; Wang, R. Impact of Urban Morphology on the Microclimate around Elementary Schools: A Case Study from Japan. *Build. Environ.* **2021**, *206*, 108383. [[CrossRef](#)]
- Nasrollahi, N.; Namazi, Y.; Taleghani, M. The Effect of Urban Shading and Canyon Geometry on Outdoor Thermal Comfort in Hot Climates: A Case Study of Ahvaz, Iran. *Sustain. Cities Soc.* **2021**, *65*, 102638. [[CrossRef](#)]
- Bouketta, S.; Bouchahm, Y. Numerical Evaluation of Urban Geometry's Control of Wind Movements in Outdoor Spaces during Winter Period. *Case of Mediterranean Climate. Renew. Energy* **2020**, *146*, 1062–1069. [[CrossRef](#)]
- Chatzidimitriou, A.; Yannas, S. Street Canyon Design and Improvement Potential for Urban Open Spaces; the Influence of Canyon Aspect Ratio and Orientation on Microclimate and Outdoor Comfort. *Sustain. Cities Soc.* **2017**, *33*, 85–101. [[CrossRef](#)]
- Muniz-Gaal, L.P.; Pezzuto, C.C.; de Carvalho, M.F.H.; Mota, L.T.M. Urban Geometry and the Microclimate of Street Canyons in Tropical Climate. *Build. Environ.* **2020**, *169*, 106547. [[CrossRef](#)]
- Hang, J.; Sandberg, M.; Li, Y.; Claesson, L. Flow Mechanisms and Flow Capacity in Idealized Long-Street City Models. *Build. Environ.* **2010**, *45*, 1042–1053. [[CrossRef](#)]
- Tong, S.; Wong, N.H.; Jusuf, S.K.; Tan, C.L.; Wong, H.F.; Ignatius, M.; Tan, E. Study on Correlation between Air Temperature and Urban Morphology Parameters in Built Environment in Northern China. *Build. Environ.* **2018**, *127*, 239–249. [[CrossRef](#)]
- He, B.J.; Ding, L.; Prasad, D. Outdoor Thermal Environment of an Open Space under Sea Breeze: A Mobile Experience in a Coastal City of Sydney, Australia. *Urban Clim.* **2020**, *31*, 100567. [[CrossRef](#)]
- Li, Y.; Song, Y. Optimization of Vegetation Arrangement to Improve Microclimate and Thermal Comfort in an Urban Park. *Int. Rev. Spat. Plan. Sustain. Dev.* **2019**, *7*, 18–30. [[CrossRef](#)]
- Armson, D.; Stringer, P.; Ennos, A.R. The Effect of Tree Shade and Grass on Surface and Globe Temperatures in an Urban Area. *Urban For. Urban Green.* **2012**, *11*, 245–255. [[CrossRef](#)]
- Lin, T.P.; Tsai, K.T.; Liao, C.C.; Huang, Y.C. Effects of Thermal Comfort and Adaptation on Park Attendance Regarding Different Shading Levels and Activity Types. *Build. Environ.* **2013**, *59*, 599–611. [[CrossRef](#)]
- Duarte, D.H.S.; Shinzato, P.; dos Santos Gusson, C.; Alves, C.A. The Impact of Vegetation on Urban Microclimate to Counterbalance Built Density in a Subtropical Changing Climate. *Urban Clim.* **2015**, *14*, 224–239. [[CrossRef](#)]
- Palme, M.; Privitera, R.; La Rosa, D. The Shading Effects of Green Infrastructure in Private Residential Areas: Building Performance Simulation to Support Urban Planning. *Energy Build.* **2020**, *229*, 110531. [[CrossRef](#)]

23. Oliveira, S.; Andrade, H.; Vaz, T. The Cooling Effect of Green Spaces as a Contribution to the Mitigation of Urban Heat: A Case Study in Lisbon. *Build. Environ.* **2011**, *46*, 2186–2194. [[CrossRef](#)]
24. Perini, K.; Chokhachian, A.; Auer, T. *Green Streets to Enhance Outdoor Comfort*; Elsevier Inc.: Amsterdam, The Netherlands, 2018; ISBN 9780128123249.
25. Jin, H.; Shao, T.; Zhang, R. Effect of Water Body Forms on Microclimate of Residential District. *Energy Procedia* **2017**, *134*, 256–265. [[CrossRef](#)]
26. Salata, F.; Golasi, I.; Vollaro, A.D.L.; Vollaro, R.D.L. How High Albedo and Traditional Buildings' Materials and Vegetation Affect the Quality of Urban Microclimate. A Case Study. *Energy Build.* **2015**, *99*, 32–49. [[CrossRef](#)]
27. Well, F.; Ludwig, F. Blue–Green Architecture: A Case Study Analysis Considering the Synergetic Effects of Water and Vegetation. *Front. Archit. Res.* **2019**, *9*, 191–202. [[CrossRef](#)]
28. Santamouris, M. Cooling the Cities—A Review of Reflective and Green Roof Mitigation Technologies to Fight Heat Island and Improve Comfort in Urban Environments. *Sol. Energy* **2014**, *103*, 682–703. [[CrossRef](#)]
29. Watanabe, S.; Nagano, K.; Ishii, J.; Horikoshi, T. Evaluation of Outdoor Thermal Comfort in Sunlight, Building Shade, and Pergola Shade during Summer in a Humid Subtropical Region. *Build. Environ.* **2014**, *82*, 556–565. [[CrossRef](#)]
30. Liu, W.; Zhang, Y.; Deng, Q. The Effects of Urban Microclimate on Outdoor Thermal Sensation and Neutral Temperature in Hot-Summer and Cold-Winter Climate. *Energy Build.* **2016**, *128*, 190–197. [[CrossRef](#)]
31. Chen, X.; Gao, L.; Xue, P.; Du, J.; Liu, J. Investigation of Outdoor Thermal Sensation and Comfort Evaluation Methods in Severe Cold Area. *Sci. Total Environ.* **2020**, *749*, 141520. [[CrossRef](#)]
32. Yang, X.; Li, Y.; Yang, L. Predicting and Understanding Temporal 3D Exterior Surface Temperature Distribution in an Ideal Courtyard. *Build. Environ.* **2012**, *57*, 38–48. [[CrossRef](#)]
33. Xu, M.; Hong, B.; Mi, J.; Yan, S. Outdoor Thermal Comfort in an Urban Park during Winter in Cold Regions of China. *Sustain. Cities Soc.* **2018**, *43*, 208–220. [[CrossRef](#)]
34. Nikolopoulou, M.; Lykoudis, S. Thermal Comfort in Outdoor Urban Spaces: Analysis across Different European Countries. *Build. Environ.* **2006**, *41*, 1455–1470. [[CrossRef](#)]
35. Dardir, M.; Berardi, U. Development of Microclimate Modeling for Enhancing Neighborhood Thermal Performance through Urban Greenery Cover. *Energy Build.* **2021**, *252*, 111428. [[CrossRef](#)]
36. Berry, R.; Livesley, S.J.; Aye, L. Tree Canopy Shade Impacts on Solar Irradiance Received by Building Walls and Their Surface Temperature. *Build. Environ.* **2013**, *69*, 91–100. [[CrossRef](#)]
37. De Abreu-Harbach, L.V.; Labaki, L.C.; Matzarakis, A. Effect of Tree Planting Design and Tree Species on Human Thermal Comfort in the Tropics. *Landsc. Urban Plan.* **2015**, *138*, 99–109. [[CrossRef](#)]
38. Morakinyo, T.E.; Kong, L.; Lau, K.K.L.; Yuan, C.; Ng, E. A Study on the Impact of Shadow-Cast and Tree Species on in-Canyon and Neighborhood's Thermal Comfort. *Build. Environ.* **2017**, *115*, 1–17. [[CrossRef](#)]
39. Hsieh, C.M.; Li, J.J.; Zhang, L.; Schwegler, B. Effects of Tree Shading and Transpiration on Building Cooling Energy Use. *Energy Build.* **2018**, *159*, 382–397. [[CrossRef](#)]
40. Xu, M.; Hong, B.; Jiang, R.; An, L.; Zhang, T. Outdoor Thermal Comfort of Shaded Spaces in an Urban Park in the Cold Region of China. *Build. Environ.* **2019**, *155*, 408–420. [[CrossRef](#)]
41. Shashua-Bar, L.; Tsiros, I.X.; Hoffman, M.E. A Modeling Study for Evaluating Passive Cooling Scenarios in Urban Streets with Trees. Case Study: Athens, Greece. *Build. Environ.* **2010**, *45*, 2798–2807. [[CrossRef](#)]
42. Sabrin, S.; Karimi, M.; Nazari, R.; Pratt, J.; Bryk, J. Effects of Different Urban-Vegetation Morphology on the Canopy-Level Thermal Comfort and the Cooling Benefits of Shade Trees: Case-Study in Philadelphia. *Sustain. Cities Soc.* **2021**, *66*, 102684. [[CrossRef](#)]
43. Feng, L.; Yang, S.; Zhou, Y.; Shuai, L. Exploring the Effects of the Spatial Arrangement and Leaf Area Density of Trees on Building Wall Temperature. *Build. Environ.* **2021**, *205*, 108295. [[CrossRef](#)]
44. Salim, S.M.; Cheah, S.C.; Chan, A. Numerical Simulation of Dispersion in Urban Street Canyons with Avenue-like Tree Plantings: Comparison between RANS and LES. *Build. Environ.* **2011**, *46*, 1735–1746. [[CrossRef](#)]
45. Park, M.; Hagishima, A.; Tanimoto, J.; Narita, K. Effect of Urban Vegetation on Outdoor Thermal Environment: Field Measurement at a Scale Model Site. *Build. Environ.* **2012**, *56*, 38–46. [[CrossRef](#)]
46. Tan, Z.; Lau, K.K.L.; Ng, E. Urban Tree Design Approaches for Mitigating Daytime Urban Heat Island Effects in a High-Density Urban Environment. *Energy Build.* **2016**, *114*, 265–274. [[CrossRef](#)]
47. Abdi, B.; Hami, A.; Zarehaghi, D. Impact of Small-Scale Tree Planting Patterns on Outdoor Cooling and Thermal Comfort. *Sustain. Cities Soc.* **2020**, *56*, 102085. [[CrossRef](#)]
48. Zhao, Y.; Chen, Y.; Li, K. A Simulation Study on the Effects of Tree Height Variations on the Façade Temperature of Enclosed Courtyard in North China. *Build. Environ.* **2022**, *207*, 108566. [[CrossRef](#)]
49. Brozovsky, J.; Corio, S.; Gaitani, N.; Gustavsen, A. Evaluation of Sustainable Strategies and Design Solutions at High-Latitude Urban Settlements to Enhance Outdoor Thermal Comfort. *Energy Build.* **2021**, *244*, 111037. [[CrossRef](#)]
50. Skelhorn, C.; Lindley, S.; Levermore, G. The Impact of Vegetation Types on Air and Surface Temperatures in a Temperate City: A Fine Scale Assessment in Manchester, UK. *Landsc. Urban Plan.* **2014**, *121*, 129–140. [[CrossRef](#)]

-
51. Perini, K.; Chokhachian, A.; Dong, S.; Auer, T. Modeling and Simulating Urban Outdoor Comfort: Coupling ENVI-Met and TRNSYS by Grasshopper. *Energy Build.* **2017**, *152*, 373–384. [[CrossRef](#)]
 52. Labdaoui, K.; Mazouz, S.; Reiter, S.; Teller, J. Thermal Perception in Outdoor Urban Spaces under the Mediterranean Climate of Annaba, Algeria. *Urban Clim.* **2021**, *39*, 100970. [[CrossRef](#)]